Bounding the Distance between a Loop Subdivision Surface and Its Limit Mesh

Zhangjin Huang and Guoping Wang

School of Electronic Engineering and Computer Science,
Peking University, Beijing 100871, China
zhangjin.huang@gmail.com
http://www.graphics.pku.edu.cn

Abstract. Given a control mesh of a Loop subdivision surface, by pushing the control vertices to their limit positions, a *limit mesh* of the Loop surface is obtained. Compared with the control mesh, the limit mesh is a tighter linear approximation in general, which inscribes the limit surface. We derive an upper bound on the distance between a Loop subdivision surface patch and its limit triangle in terms of the maximum norm of the mixed second differences of the initial control vertices and a constant that depends only on the valence of the patch's extraordinary vertex. A subdivision depth estimation formula for the limit mesh approximation is also proposed.

Key words: Loop subdivision surfaces, Limit mesh, Error bound, Subdivision depth

1 Introduction

A subdivision surface is defined as the limit of a sequence of successively refined control meshes. In practice such as surface rendering, surface trimming and surface intersection, a linear approximation (for example, a refined control mesh) is used to substitute the smooth surface. It is natural to ask the following questions: How does one estimate the *error (distance)* between a limit surface and its linear approximation (for instance, the control mesh)? How many steps of subdivision would be necessary to satify a user-specified error tolerance?

Loop subdivision surfaces generalize the quartic three-directional box spline surfaces to triangular meshes of arbitrary topology [1]. Several works have been devoted to studying the distance between a Loop surface and its control mesh approximation [2–6]. These error estimation techniques can be classified into two classes.

One is the vertex based method [2, 3], which measures the distance between the control vertices and their limit positions. In [2], Lanquetin et al. derived a wrong exponential bound which resulted in a improper subdivision depth formula. In [3], Wang et al. proposed a proper exponential bound with an awkward subdivision depth estimation technique. The vertex based bounds all suffer from

one problem as pointed out in [3]: they may be smaller than the actual maximal distance between the limit surface and its control mesh in some cases. The other is the patch based method [4–6], which estimates the parametric distance between a Loop surface patch and its control mesh. Wu et al. presented an accurate error measure for adaptive subdivision and interference detection [4, 5]. But their estimate is dependent on recursive subdivision, thus can not be used to pre-compute the error bound after n steps of subdivision or predict the recursion depth within a user-specified tolerance. In [6], Huang derived a bound in terms of the maximum norm of the mixed second differences of the initial control vertices, and a subdivision depth estimation approach.

The *limit mesh* of a Loop surface, obtained by pushing the control vertices of its control mesh to their limit positions, has been applied in surface reconstruction [8]. The limit mesh is usually considered a better linear approximation than the corresponding control mesh. But the approximation error for Loop surfaces has not been investigated yet. Recently, an effective approach has been proposed to bound the error of the limit mesh approximation to a Catmull-Clark subdivision surface [7]. With an analogous technique, in this paper we derive a bound on the maximum distance between a Loop surface patch and its limit triangle. The bound is expressed in terms of the maximum norm of the mixed second differences of the Loop patch's initial control mesh and a constant that depends only on the valence of the patch's extraordinary vertex.

The paper is organized as follows. Section 2 introduces some definitions and notations. In Sections 3 and 4, we derive distance bounds for regular Loop patches and extraordinary Loop patches, respectively. And a subdivision depth estimation method for the limit mesh approximation is presented in Section 5. In Section 6, we compare the limit mesh approximation with the control mesh approximation. Finally we conclude the paper with some suggestions for future work.

2 Definition and Notation

Without loss of generality, we assume the initial control mesh has been subdivided at least once, isolating the extraordinary vertices so that each face is a triangle and contains at most one extraordinary vertex.

2.1 Distance

Given a control mesh of a Loop subdivision surface $\tilde{\mathbf{S}}$, for each interior triangle $\mathbf{F}$ in the control mesh, there is a corresponding *limit triangle* $\overline{\mathbf{F}}$ in the limit mesh, and a corresponding surface patch $\mathbf{S}$ in the limit surface $\tilde{\mathbf{S}}$. Obviously, the limit triangle $\overline{\mathbf{F}}$ is the triangle formed by connecting the three corner points of $\mathbf{S}$.

The *distance* between a Loop patch $\mathbf{S}$ and the corresponding limit triangle $\overline{\mathbf{F}}$ is defined as the maximum distance between $\mathbf{S}(v, w)$ and $\overline{\mathbf{F}}(v, w)$, that is,

$$\max_{(v,w)\in\Omega} \|\mathbf{S}(v, w) - \overline{\mathbf{F}}(v, w)\| \ ,$$

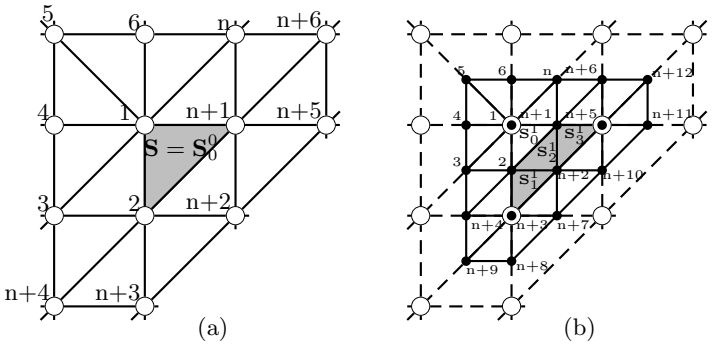

Fig. 1. (a) Ordering of the control vertices of an extraordinary patch $\mathbf{S}$ of valence n. (b) Ordering of the new control vertices (*solid dots*) after one step of Loop subdivision.

where Ω is the unit triangle, $\mathbf{S}(v, w)$ is the Stam's parametrization [9] of $\mathbf{S}$ over Ω, and $\overline{\mathbf{F}}(v, w)$ is the linear parametrization of $\overline{\mathbf{F}}$ over Ω.

2.2 Second Order Norm

The control mesh Π of a Loop patch $\mathbf{S}$ consists of $n + 6$ control vertices $\Pi = \{\mathbf{P}_i : i = 1, 2, \ldots, n+6\}$, where n is the valence of $\mathbf{F}$'s only extraordinary vertex (if has, otherwise $n = 6$) and called the *valence* of the patch $\mathbf{S}$ (see Figure 1(a)).

The *second order norm* of Π, denoted $M = M^0 = M_0^0$, is defined as the maximum norm of the following $n + 9$ mixed second differences (MSDs) $\{\alpha_i : 1 \le i \le n + 9\}$ of the $n + 6$ vertices of Π:

$$\begin{aligned} M = \max\{&\|\mathbf{P}_1 + \mathbf{P}_2 - \mathbf{P}_{n+1} - \mathbf{P}_3\|, \{\|\mathbf{P}_1 + \mathbf{P}_i - \mathbf{P}_{i-1} - \mathbf{P}_{i+1}\| : 3 \le i \le n\}, \\ &\|\mathbf{P}_1 + \mathbf{P}_{n+1} - \mathbf{P}_n - \mathbf{P}_2\|, \|\mathbf{P}_2 + \mathbf{P}_{n+1} - \mathbf{P}_1 - \mathbf{P}_{n+2}\|, \\ &\|\mathbf{P}_2 + \mathbf{P}_{n+2} - \mathbf{P}_{n+1} - \mathbf{P}_{n+3}\|, \|\mathbf{P}_2 + \mathbf{P}_{n+3} - \mathbf{P}_{n+2} - \mathbf{P}_{n+4}\|, \\ &\|\mathbf{P}_2 + \mathbf{P}_{n+4} - \mathbf{P}_{n+3} - \mathbf{P}_3\|, \|\mathbf{P}_2 + \mathbf{P}_3 - \mathbf{P}_{n+4} - \mathbf{P}_1\|, \\ &\|\mathbf{P}_{n+1} + \mathbf{P}_n - \mathbf{P}_1 - \mathbf{P}_{n+6}\|, \|\mathbf{P}_{n+1} + \mathbf{P}_{n+6} - \mathbf{P}_n - \mathbf{P}_{n+5}\|, \\ &\|\mathbf{P}_{n+1} + \mathbf{P}_{n+5} - \mathbf{P}_{n+6} - \mathbf{P}_{n+2}\|, \|\mathbf{P}_{n+1} + \mathbf{P}_{n+2} - \mathbf{P}_{n+5} - \mathbf{P}_2\|\} \\ = \max\{&\|\alpha_i\| : i = 1, \ldots, n + 9\} \ . \end{aligned} \tag{1}$$

M is also called the (level-0) second order norm of the patch $\mathbf{S}$. For a regular patch ($n = 6$), there are 15 mixed second differences.

Through subdivision we can generate $n+12$ new vertices $\mathbf{P}_i^1$, $i = 1, \ldots, n+12$ (see Figure 1(b)), which are called the level-1 control vertices of $\mathbf{S}$. All these level-1 control vertices compose $\mathbf{S}$'s level-1 control mesh $\Pi^1 = \{\mathbf{P}_i^1 : i = 1, 2, \ldots, n + 12\}$. We use $\mathbf{P}_i^k$ and Π^k to represent the level-k control vertices and level-k control mesh of $\mathbf{S}$, respectively, after k steps of subdivision on Π.

The level-1 control vertices form four control vertex sets $\Pi_0^1, \Pi_1^1, \Pi_2^1$ and Π_3^1, corresponding to the control meshes of the subpatches $\mathbf{S}_0^1, \mathbf{S}_1^1, \mathbf{S}_2^1$ and $\mathbf{S}_3^1$,

respectively (see Figure 1b), where $\Pi_0^1 = \{P_i^1 : 1 \le i \le n+6\}$. The subpatch $\mathbf{S}_0^1$ is an extraordinary patch, but $\mathbf{S}_1^1, \mathbf{S}_2^1$ and $\mathbf{S}_3^1$ are regular triangular patches [9]. Following the definition in Equation (1), one can define the second order norms M_i^1 for $\mathbf{S}_i^1, i = 0, 1, 2, 3$, respectively. $M^1 = \max\{M_i^1 : i = 0, 1, 2, 3\}$ is defined as the second order norm of the level-1 control mesh Π^1. After k steps of subdivision on Π, one gets 4^k control point sets $\Pi_i^k : i = 0, 1, \ldots, 4^k - 1$ corresponding to the 4^k subpatches $\mathbf{S}_i^k : i = 0, 1, \ldots, 4^k - 1$ of $\mathbf{S}$, with $\mathbf{S}_0^k$ being the only level-k extraordinary patch (if $n \neq 6$). We denote M_i^k and M^k as the second order norms of Π_i^k and Π^k, respectively.

3 Regular Patch

In this section, both the regular Loop patch $\mathbf{S}$ and its corresponding limit triangle $\overline{\mathbf{F}}$ are first expressed in quartic triangular Bézier form. Then we bound the distance between $\mathbf{S}$ and $\overline{\mathbf{F}}$ by measuring the deviations between their corresponding Bézier points.

3.1 Quartic Triangular Bézier Form

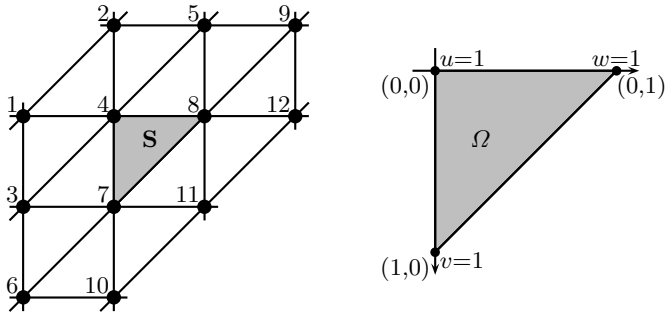

Fig. 2. Control vertices of a quartic box spline patch and their ordering.

If $\mathbf{S}$ is a regular Loop patch, then $\mathbf{S}(u, v)$ can be expressed as a quartic box spline patch defined by 12 control vertices $\mathbf{p}_i, 1 \le i \le 12$ (see Figure 2):

$$\mathbf{S}(v, w) = \sum_{i=1}^{12} \mathbf{p}_i N_i(v, w), \quad (v, w) \in \Omega \ , \tag{2}$$

where $N_i(v, w), 1 \le i \le 12$ are the quartic box spline basis functions. The expressions of $N_i(v, w)$ refer to [9]. The surface is defined over the unit triangle:

$$\Omega = \{(v, w) \,|\, v \in [0, 1] \text{ and } w \in [0, 1 - v]\} \ .$$

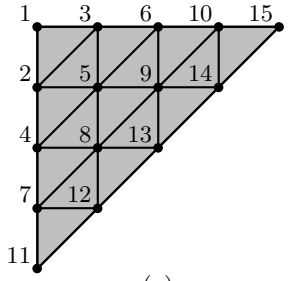

(a)

$$u^4 \quad 4u^3w \quad 6u^2w^2 \quad 4uw^3 \quad w^4$$
$$4u^3v \quad 12u^2vw \quad 12uvw^2 \quad 4vw^3$$
$$6u^2v^2 \quad 12uv^2w \quad 6v^2w^2$$
$$4uv^3 \quad 4v^3w$$
$$v^4$$

(b)

Fig. 3. (a) Ordering of the Bézier points of a quartic triangular Bézier patch. (b) Quartic Bernstein polynomials corresponding to the Bézier points.

We introduce the third parameter $u = 1 - v - w$ such that (u, v, w) forms a barycentric system of coordinates for the unit triangle.

$\mathbf{S}$ is a quartic triangular Bézier patch, thus $\mathbf{S}(u, v)$ can be written in terms of Bernstein polynomials [11]:

$$\mathbf{S}(u,v) = \sum_{i=1}^{15} \mathbf{b}_i B_i(v,w), \quad (v,w) \in \Omega \ , \tag{3}$$

where $\mathbf{b}_i, 1 \le i \le 15$ are the Bézier points of $\mathbf{S}$, and $B_i(v,w), 1 \le i \le 15$ are the quartic Bernstein polynomials (see Figure 3). The correspondence between the standard representation $B^4_{ijk}(u,v,w) = \frac{4!}{i!j!k!}u^i v^j w^k$, $i,j,k \ge 0$, $i+j+k=4$ and $B_i(v,w), 1 \le i \le 15$ is $(i,j,k) \mapsto \frac{(j+k)(j+k+1)}{2} + k + 1$. With the algorithm developed in [10], we can get the 15×12 matrix T which converts from the 12 control vertices $(\mathbf{p}_i)$ to the 15 Bézier points $(\mathbf{b}_i)$ (see Appendix 1).

Note that $\overline{\mathbf{F}} = \{\mathbf{b}_1, \mathbf{b}_{11}, \mathbf{b}_{15}\}$ is the limit triangle corresponding to the center triangle $\mathbf{F} = \{\mathbf{p}_4, \mathbf{p}_7, \mathbf{p}_8\}$ (see Figures 2 and 3). The linear parametrization of $\overline{\mathbf{F}}$ is

$$\overline{\mathbf{F}}(v,w) = u\mathbf{b}_1 + v\mathbf{b}_{11} + w\mathbf{b}_{15} \ ,$$

where $u = 1-v-w$. By the linear precision property of the Bernstein polynomials [11], we can express $\overline{\mathbf{F}}(v,w)$ as the following quartic Bézier form:

$$\overline{\mathbf{F}}(v,w) = \sum_{i=1}^{15} \overline{\mathbf{b}}_i B_i(v,w) \ , \tag{4}$$

where $\overline{\mathbf{b}}_{\frac{(j+k)(j+k+1)}{2}+k+1} = \overline{\mathbf{F}}(\frac{j}{4}, \frac{k}{4})$, $j,k \ge 0$, $0 \le j+k \le 4$ are the Bézier points.

3.2 Bounding the Distance

According to the previous analysis, for $(v,w) \in \Omega$, it follows that

$$\|\mathbf{S}(v,w) - \overline{\mathbf{F}}(v,w)\| = \left\| \sum_{i=1}^{15} (\mathbf{b}_i - \overline{\mathbf{b}}_i) B_i(v,w) \right\| \le \sum_{i=1}^{15} \|\mathbf{b}_i - \overline{\mathbf{b}}_i\| B_i(v,w) \ . \tag{5}$$

In the following, we compute the smallest possible constants $\delta_i, i = 1, 2, \ldots, 15$ such that $\|\mathbf{b}_i - \overline{\mathbf{b}}_i\|$ is bounded by

$$\|\mathbf{b}_i - \overline{\mathbf{b}}_i\| \leq \delta_i M \ ,$$

where M is the second order norm of $\mathbf{S}$. It is obvious that $\delta_1 = \delta_{11} = \delta_{15} = 0$. $\mathbf{b}_i$ and $\overline{\mathbf{b}}_i, 1 \leq i \leq 15$ are the convex combinations of the control vertices $\mathbf{p}_i, i = 1, 2, \ldots, 12$, and $\mathbf{b}_i - \overline{\mathbf{b}}_i$ can be expressed as a linear combination of the 15 MSDs $\alpha_l, l = 1, 2, \ldots 15$ defined in Equation (1) as follows:

$$\mathbf{b}_i - \overline{\mathbf{b}}_i = \sum_{l=1}^{15} x_l^i \alpha_l \ ,$$

where $x_l^i, l = 1, 2, \ldots, 15$ are undetermined real coefficients. It follows that

$$\|\mathbf{b}_i - \overline{\mathbf{b}}_i\| \leq \sum_{l=1}^{15} \|x_l^i \alpha_l\| \leq \sum_{l=1}^{15} |x_l^i| \|\alpha_l\| \leq \sum_{l=1}^{15} |x_l^i| M \ .$$

Therefore, to get a tight upper bound for $\|\mathbf{b}_i - \overline{\mathbf{b}}_i\|$, we solve the following constrained minimization problem:

$$\begin{aligned} \delta_i &= \min \sum_{l=1}^{15} |x_l^i| \\ s.t. \quad & \sum_{l=1}^{15} x_l^i \alpha_l = \mathbf{b}_i - \overline{\mathbf{b}}_i \ . \end{aligned} \tag{6}$$

By symmetry, we only need to solve three constrained minimization problems. With the help of the symbolic computation of *Mathematica*, we have

$$\begin{aligned} &\delta_1 = \delta_{11} = \delta_{15} = 0 \ , \\ &\delta_2 = \delta_3 = \delta_7 = \delta_{10} = \delta_{12} = \delta_{14} = \frac{1}{4} \ , \\ &\delta_4 = \delta_6 = \delta_{13} = \frac{1}{3} \ , \\ &\delta_5 = \delta_8 = \delta_9 = \frac{5}{12} \ . \end{aligned}$$

It follows that

$$\mathcal{B}(v, w) = \sum_{i=1}^{15} \delta_i B_i(v, w) = v + w - v^2 - vw - w^2 \ .$$

We obtain a bound on the pointwise distance between $\mathbf{S}(v, w)$ and $\overline{\mathbf{F}}(v, w)$:

Theorem 1. *For $(v, w) \in \Omega$, we have*

$$\|\mathbf{S}(v, w) - \overline{\mathbf{F}}(v, w)\| \leq \mathcal{B}(v, w) M \ ,$$

where $\mathcal{B}(v, w) = v + w - v^2 - vw - w^2$ is called the distance bound function *of $\mathbf{S}(v, w)$ with respect to $\overline{\mathbf{F}}(v, w)$.*

By symmetry, the maximum of $\mathcal{B}(u,v), (u,v) \in \Omega$ must occur on the diagonal $\mathcal{B}(t,t) = 2t - 3t^2, 0 \le t \le \frac{1}{2}$. Since

$$\max_{0 \le t \le 1/2} 2t - 3t^2 = \frac{1}{3} = \mathcal{B}(\frac{1}{3}, \frac{1}{3}) \ ,$$

we have a bound on the maximal distance between $\mathbf{S}(u,v)$ and $\overline{\mathbf{F}}(u,v)$ as stated in the following theorem:

Theorem 2. *The distance between a regular Loop patch* $\mathbf{S}$ *and the corresponding limit triangle* $\overline{\mathbf{F}}$ *is bounded by*

$$\max_{(v,w) \in \Omega} \|\mathbf{S}(v,w) - \overline{\mathbf{F}}(v,w)\| \le \frac{1}{3} M \ .$$

4 Extraordinary Patch

For an extraordinary patch, we first partition it into regular triangular subpatches with Stam's parametrization [9], then derive a distance bound function for each regular subpatch with the technique developed in Section 3.

4.1 Stam's Parametrization

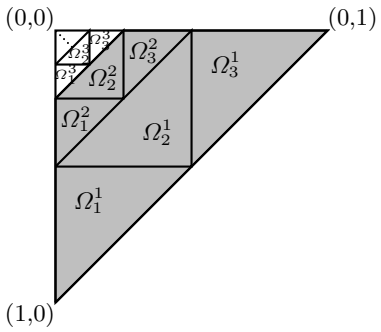

Fig. 4. Partition of the parameter domain Ω.

Through subdivision an extraordinary Loop patch $\mathbf{S}$ of valence n can be partitioned into an infinite sequence of regular triangular patches $\{\mathbf{S}_m^k\}, k \ge 1, m = 1,2,3$. If we partition the unit triangle Ω into an infinite set of tiles $\{\Omega_m^k\}, k \ge 1, m = 1,2,3$ (see Figure 4), accordingly, with

$$\begin{aligned}
\Omega_1^k &= \{(v,w) \,|\, v \in [2^{-k}, 2^{-k+1}] \text{ and } w \in [0, 2^{-k+1} - v]\} \ , \\
\Omega_2^k &= \{(v,w) \,|\, v \in [0, 2^{-k}] \text{ and } w \in [2^{-k} - v, 2^{-k}]\} \ , \\
\Omega_3^k &= \{(v,w) \,|\, v \in [0, 2^{-k}] \text{ and } w \in [2^{-k}, 2^{-k+1} - v]\} \ .
\end{aligned}$$

Each tile Ω_m^k corresponds to a box spline patch $\mathbf{S}_m^k$. And $\mathbf{S}_m^k(v,w)$ is defined over the unit triangle with the form as Equation (2). Therefore, the parametrization for $\mathbf{S}(v,w)$ is constructed as follows [9]:

$$\mathbf{S}(v,w) \mid_{\Omega_m^k} = \mathbf{S}_m^k(\tilde{v},\tilde{w}) = \mathbf{S}_m^k(\mathbf{t}_m^k(v,w)) \ ,$$

where the transformation $\mathbf{t}_m^k$ maps the tile Ω_m^k onto the unit triangle Ω.

The center triangle of $\mathbf{S}$'s control mesh is $\mathbf{F} = \{\mathbf{P}_1, \mathbf{P}_2, \mathbf{P}_{n+1}\}$ (see Figure 1), and the corresponding limit triangle is $\overline{\mathbf{F}} = \{\overline{\mathbf{P}}_1, \overline{\mathbf{P}}_2, \overline{\mathbf{P}}_{n+1}\}$, with $\overline{\mathbf{P}}_i$ being the limit point of $\mathbf{P}_i, i = 1, 2, n+1$. Let $\overline{\mathbf{F}}(u,v)$ be the linear parametrization of $\overline{\mathbf{F}}$:

$$\overline{\mathbf{F}}(v,w) = u\overline{\mathbf{P}}_1 + v\overline{\mathbf{P}}_2 + w\overline{\mathbf{P}}_{n+1}, \quad (v,w) \in \Omega \ . \tag{7}$$

The limit triangle $\overline{\mathbf{F}}$ can be partitioned into sub-triangles defined over Ω_m^k as follows:

$$\overline{\mathbf{F}}(v,w) \mid_{\Omega_m^k} = \widehat{\mathbf{F}}_m^k(\mathbf{t}_m^k(v,w))) \ .$$

Here $\widehat{\mathbf{F}}_m^k$ is the linear patch defined as

$$\widehat{\mathbf{F}}_m^k(v,w) = u\overline{\mathbf{b}}_1 + v\overline{\mathbf{b}}_{11} + w\overline{\mathbf{b}}_{15}, \quad (v,w) \in \Omega \ . \tag{8}$$

If the three corners of Ω_m^k are $(v_1,w_1), (v_2,w_2)$ and (v_3,w_3), which correspond to $(0,0), (1,0)$ and $(0,1)$ in Ω via the transformation $\mathbf{t}_m^k$, respectively. Then

$$\overline{\mathbf{b}}_1 = \overline{\mathbf{F}}(v_1,w_1) \ , \quad \overline{\mathbf{b}}_{11} = \overline{\mathbf{F}}(v_2,w_2) \ , \quad \overline{\mathbf{b}}_{15} = \overline{\mathbf{F}}(v_3,w_3) \ .$$

4.2 Bounding the Distance

Similar to the analysis in Section 3, we can rewrite $\mathbf{S}_m^k(v,w)$ and $\widehat{\mathbf{F}}_m^k(v,w)$ into the quartic Bézier forms as Equations (3) and (4), respectively. Thus for $(v,w) \in \Omega_m^k$, we have

$$\|\mathbf{S}(v,w) - \overline{\mathbf{F}}(v,w)\| = \|\mathbf{S}_m^k(\tilde{v},\tilde{w}) - \widehat{\mathbf{F}}_m^k(\tilde{v},\tilde{w})\| \leq \sum_{i=1}^{15} \|\mathbf{b}_i - \overline{\mathbf{b}}_i\| B_i(\tilde{v},\tilde{w}). \tag{9}$$

Notice that $\widehat{\mathbf{F}}_m^k$ is not the limit triangle of the triangular patch $\mathbf{S}_m^k$ but one portion of the extraordinary patch $\mathbf{S}$'s limit triangle $\overline{\mathbf{F}}$. So we can not use the results for $\|\mathbf{b}_i - \overline{\mathbf{b}}_i\|$ derived in Section 3 directly.

By solving 15 constrained minimization problems with the form similar to Equation (6), we have

$$\|\mathbf{b}_i - \overline{\mathbf{b}}_i\| \leq \delta_i M, \ 1 \leq i \leq 15 \ .$$

Consequently, it follows from Equation (9) that

$$\|\mathbf{S}_m^k(v,w) - \widehat{\mathbf{F}}_m^k(v,w)\| \leq \mathcal{B}_m^k(v,w) M, \ (v,w) \in \Omega \ ,$$

where the quartic Bézier function

$$\mathcal{B}_m^k(v,w) = \sum_{i=1}^{15} \delta_i B_i(v,w),\ (v,w) \in \Omega \tag{10}$$

is the *distance bound function* of $\mathbf{S}_m^k(v,w)$ with respect to $\widehat{\mathbf{F}}_m^k(v,w)$. Then the *distance bound function* of $\mathbf{S}(v,w)$ with respect to $\overline{\mathbf{F}}(v,w)$, $\mathcal{B}(v,w), (v,w) \in \Omega$, can be defined as follows:

$$\mathcal{B}(v,w) \mid_{\Omega_m^k} = \mathcal{B}_m^k(\mathbf{t}_m^k(v,w)),\ k \geq 1, m = 1,2,3\ .$$

It is obvious that $\mathcal{B}(0,0) = \mathcal{B}(1,0) = \mathcal{B}(0,1) = 0$, and $\mathcal{B}(v,w)$ is a piecewise quartic triangular Bézier function over Ω away from $(0,0)$. Let $\beta(n) = \max_{(v,w)\in\Omega} \mathcal{B}(v,w)$, we have the following theorem on the maximal distance between $\mathbf{S}(v,w)$ and $\overline{\mathbf{F}}(v,w)$:

Theorem 3. *The distance between an extraordinary Loop patch* $\mathbf{S}$ *of valence* n *and the corresponding limit face* $\overline{\mathbf{F}}$ *is bounded by*

$$\max_{(v,w)\in\Omega} \|\mathbf{S}(v,w) - \overline{\mathbf{F}}(v,w)\| \leq \beta(n) M\ , \tag{11}$$

where $\beta(n)$ is a constant that depends only on n, the valence of $\mathbf{S}$.

For $3 \leq n \leq 50$, we investigate the maximums of the quartic Bézier functions $\mathcal{B}_m^k(v,w), k \geq 1, m = 1,2,3$ over Ω assisted by plotting the graph of $\mathcal{B}(v,w)$. The following facts are found:

1. $\mathcal{B}(v,w)$ attains its maximum in the domain $\overline{\Omega} = \Omega \cap \{(v,w) \mid v + w \geq \frac{1}{4}\}$ (shaded region in Figure 4).
2. $\mathcal{B}(v,w)$ attains its maximum either on the diagonal $\mathcal{B}(t,t), t \in [0, \frac{1}{2}]$ or on the borders $\mathcal{B}(t,0)$ and $\mathcal{B}(0,t), t \in [0,1]$.

By symmetry, to compute the value of $\beta(n)$, at most four distance bound functions corresponding to $\mathbf{S}_1^1, \mathbf{S}_2^1, \mathbf{S}_1^2, \mathbf{S}_2^2$ are needed to be analyzed. Numerical results for $\beta(n), 3 \leq n \leq 10$ are given in Table 2. For regular Loop patches, the constant $\beta(n) = \frac{1}{3}$ is optimum. But for extraordinary Loop patches, the constants can be improved through further subdividing the subpatches $\mathbf{S}_m^k$.

5 Subdivision Depth Estimation

Before estimating subdivision depth, we investigate the recurrence relation between the second order norms of the control meshes of $\mathbf{S}$ at different levels.

5.1 Convergence Rate of Second Order Norm

If the second order norms M_0^{k+j} and M_0^j satisfy the following recurrence inequality

$$M_0^{k+j} \leq r_j(n) M_0^k, \quad j \geq 0\ , \tag{12}$$

where $r_j(n)$ is a constant which depends on n, the valence of the extraordinary vertex, and $r_0(n) \equiv 1$. We call $r_j(n)$ the *j-step convergence rate* of second order norm. The convergence rate reflects how fast the control mesh converges to the limit surface. The smaller the convergence rate is, the faster the control mesh converges. It is obvious that $r_{j+k} \leq r_j r_k$.

Let $\alpha_i^k, i = 1, 2, \ldots, n+9$ be the MSDs of $\Pi_0^k, k \geq 0$ defined as in Equation (1). For each $l = 1, 2, \ldots, n+9$, we express α_l^{k+1} as a linear combination of α_i^k:

$$\alpha_l^{k+1} = \sum_{i=1}^{n+9} x_i^l \alpha_i^k \ ,$$

where $x_i^l, i = 1, 2, \ldots, n+9$ are undetermined real coefficients. Then we can bound $\|\alpha_l^{k+1}\|$ by $c_l(n) M_0^k$, where $c_l(n)$ is the solution of the following constrained minimization problem

$$\begin{aligned} c_l(n) &= \min \sum_{i=1}^{n+9} |x_i^l| \ , \\ s.t. \quad & \sum_{i=1}^{n+9} x_i^l \alpha_i^k = \alpha_l^{k+1} \ . \end{aligned} \tag{13}$$

Since $M_0^{k+1} = \max\{\|\alpha_l^{k+1}\| : 1 \leq l \leq n+9\}$, we get an estimate for $r_1(n)$ as follows

$$r_1(n) = \max_{1 \leq l \leq n+9} c_l(n) \ .$$

By symmetry, we only need to solve at most four constrained minimization problems corresponding to $\alpha_1^{k+1} = \mathbf{P}_1^{k+1} + \mathbf{P}_2^{k+1} - \mathbf{P}_{n+1}^{k+1} - \mathbf{P}_3^{k+1}$, $\alpha_{n+1}^{k+1} = \mathbf{P}_2 + \mathbf{P}_{n+1} - \mathbf{P}_1 - \mathbf{P}_{n+2}$, $\alpha_{n+2}^{k+1} = \mathbf{P}_2 + \mathbf{P}_{n+2} - \mathbf{P}_{n+1} - \mathbf{P}_{n+3}$, and $\alpha_{n+3}^{k+1} = \mathbf{P}_2 + \mathbf{P}_{n+3} - \mathbf{P}_{n+2} - \mathbf{P}_{n+4}$, respectively. Since $\mathbf{P}_1^{k+1}$ is the extraordinary vertex, it is not surprising to find out that $c_1(n)$ is the maximum for $n > 3$. The special case is $r_1(3) = c_4(3) = 0.4375 > c_1(3) = 0.3125$. Then it follows that

$$r_1(n) = c_1(n), \ n > 3 \ .$$

Similarly, we can estimate $r_j(n), \ n \geq 3, \ j > 1$ by solving only one constrained minimization problem (13) with α_1^{k+1} replaced by α_1^{k+j}. Then we have

Lemma 1. *If M_0^k represents the second order norm of the level-k extraordinary subpatch $S_0^k, k \geq 0$ of valence n, then it follows that*

$$M_0^{k+j} \leq r_j(n) M_0^k, \quad j \geq 1 \ .$$

The above lemma works in a more general sense, that is, if M_0^k is replaced with M^k, the second order norm of the level-k control mesh Π^k, the estimates for $r_j(n)$ still work.

Though $r_2(n)$ can be roughly estimated as $r_1(n)^2$, in practice $r_2(n)$ may derive better results than $r_1(n)^2$ as shown in the next subsection. Table 1 shows

the convergence rates $r_j(n), j = 1, 2, 3$ for $3 \leq n \leq 10$. The convergence rate $r_j(6) = (\frac{1}{4})^j$ is sharp for regular patches. $r_j(n) > r_j(6), n \neq 6$ means the control mesh near an extraordinary vertex converges to the limit surface slower than a regular mesh.

Table 1. Convergence rates $r_i(n),\ i = 1, 2, 3$

n	3	4	5	6	7	8	9	10
$r_1(n)$	0.437500	0.382813	0.540907	0.250000	0.674025	0.705136	0.726355	0.741711
$r_2(n)$	0.082031	0.142700	0.258367	0.062500	0.372582	0.402608	0.424000	0.439960
$r_3(n)$	0.020752	0.053148	0.118899	0.015625	0.197695	0.219995	0.236377	0.248872

5.2 Subdivision Depth

Given an error tolerance $\epsilon > 0$, the *subdivision depth* of a Loop patch $\mathbf{S}$ with respect to ϵ is a positive integer d such that if the control mesh of S is recursively subdivided d times, the distance between the resulting limit mesh and $\mathbf{S}$ is smaller than ϵ.

The distance between an extraordinary Loop patch $\mathbf{S}(v, w)$ and its level-1 limit mesh can be expressed as

$$\max_{i=0,1,2,3} \max_{(v,w)\in\Omega} \|\mathbf{S}_i^1(v, w) - \overline{\mathbf{F}}_i^1(v, w)\| \ ,$$

where $\mathbf{S}_i^1, i = 0, 1, 2, 3$ are the level-1 subpatches of $\mathbf{S}$ as described in Section 2.2, and $\overline{\mathbf{F}}_i^1$ are the limit triangles corresponding to $\mathbf{S}_i^1, i = 0, 1, 2, 3$, respectively. It is easy to see that

$$\max_{(v,w)\in\Omega} \|\mathbf{S}_0^1(v, w) - \overline{\mathbf{F}}_0^1(v, w)\| \leq \beta(n) M_0^1 \leq \beta(n) r_1(n) M^0 \ ,$$

$$\max_{(v,w)\in\Omega} \|\mathbf{S}_i^1(v, w) - \overline{\mathbf{F}}_i^1(v, w)\| \leq \beta(6) M_i^1 \leq \frac{1}{3} r_1(n) M^0,\ i = 1, 2, 3 \ .$$

Then it follows that

$$\max_{i=0,1,2,3} \max_{(v,w)\in\Omega} \|\mathbf{S}_i^1(v, w) - \overline{\mathbf{F}}_i^1(v, w)\| \leq \max\{\beta(n), \frac{1}{3}\} r_1(n) M^0 \ .$$

Since $r_1(n) \geq \frac{1}{4}$ and $r_{i+1}(n) \geq \frac{1}{4} r_i(n)$, the distance between an extraordinary Loop patch $\mathbf{S}(v, w)$ and its level-k limit mesh is bounded by

$$\max_{i=0,1,\ldots,4^k-1} \max_{(v,w)\in\Omega} \|\mathbf{S}_i^k(v, w) - \overline{\mathbf{F}}_i^k(v, w)\| \leq \max\{\beta(n), \frac{1}{3}\} r_k(n) M^0 \ .$$

Assume $k = \lambda l_j + j, 0 \leq j \leq \lambda - 1$, then $r_k(n) \leq (r_\lambda(n))^{l_j} r_j(n)$. Let

$$\max\{\beta(n), \frac{1}{3}\} r_k(n) M^0 \leq \max\{\beta(n), \frac{1}{3}\} (r_\lambda(n))^{l_j} r_j(n) M^0 < \epsilon \ ,$$

then it follows that $l_j \geq \left\lceil \log_{\frac{1}{r_\lambda(n)}} \left(\frac{r_j(n) \max\{\beta(n), \frac{1}{3}\} M^0}{\epsilon} \right) \right\rceil$. Consequently, we have the following subdivision depth estimation theorem for Loop patches.

Theorem 4. *Given a Loop patch* $\mathbf{S}$ *of valence* n *and an error tolerance* $\epsilon > 0$*, after*

$$k = \min_{0 \leq j \leq \lambda - 1} \lambda l_j + j \tag{14}$$

steps of subdivision on the control mesh of $\mathbf{S}$*, the distance between* $\mathbf{S}$ *and its level-*k *limit mesh is smaller than* ϵ*. Here,*

$$l_j = \left\lceil \log_{\frac{1}{r_\lambda(n)}} \left(\frac{r_j(n) \max\{\beta(n), \frac{1}{3}\} M}{\epsilon} \right) \right\rceil, \quad 0 \leq j \leq \lambda - 1, \lambda \geq 1 \ .$$

In particular, for regular Loop patches, $k = \left\lceil \log_4 \left(\frac{M}{3\epsilon} \right) \right\rceil$.

6 Comparison

Both a control mesh and its corresponding limit mesh can be employed to approximate a Loop surface in practical applications. This section compares these two approximation representations within the framework of the second order difference techniques.

The distance between a Loop patch $\mathbf{S}$ of valence n and its control mesh can be bounded in terms of the second order norm M as [6]:

$$\max_{(v,w) \in \Omega} \|\mathbf{S}(v,w) - \mathbf{F}(v,w)\| \leq C_\lambda(n) M, \quad \lambda \geq 1 \ , \tag{15}$$

where

$$C_\lambda(n) = \beta(n) \frac{\sum_{i=0}^{\lambda-1} r_i(n)}{1 - r_\lambda(n)} \ .$$

Table 2 illustrates the comparison results of the constants $C_3(n)$ and $\beta(n)$ for $3 \leq n \leq 10$. It can be seen that $C_3(6) = \frac{1}{2}$ is the smallest of $C_3(n), n \geq 3$. $\beta(n) < C_3(6), n \geq 3$ means that the limit mesh approximates a Loop surface better than the corresponding control mesh in general.

Table 2. Comparison of $C_3(n)$ and $\beta(n)$, $3 \leq n \leq 10$

n	3	4	5	6	7	8	9	10
$C_3(n)$	0.872850	0.780397	0.858623	0.500000	0.875407	0.866176	0.856245	0.847476
$\beta(n)$	0.358813	0.350722	0.342499	0.333333	0.329252	0.332001	0.333880	0.335299

Given a Loop patch $\mathbf{S}$ of valence n and an error tolerance $\epsilon > 0$, the subdivision depth estimation formula for the control mesh approximation is [6]:

$$k = \min_{0 \leq j \leq a - 1} a l_j + j \ , \tag{16}$$

where

$$l_j = \left\lceil \log_{\frac{1}{r_\lambda(n)}} \left(\frac{r_j(n) C_\lambda(n) M}{\epsilon} \right) \right\rceil, \quad 0 \le j \le \lambda - 1, \lambda \ge 1 \ .$$

For regular Loop patches, $k = \left\lceil \log_4 \left(\frac{M}{2\epsilon} \right) \right\rceil$.

Table 3 shows the comparison results of subdivision depths. The error tolerance ϵ is set to 0.0001, and the second order norm M is assumed to be 1. As can be seen from the table, the limit mesh approximation has a 20% improvement over the control mesh approximation in most of the cases.

Table 3. Comparison of subdivision depths

n	3	4	5	6	7	8	9	10
control mesh	8	10	14	7	19	21	22	23
limit mesh	7	9	12	6	16	17	18	18

7 Conclusions and Future Work

In this paper we investigate the distance (error) between a Loop subdivision surface and its limit mesh. The maximal distance between a Loop patch and its limit triangle is bounded in terms of the second order norm of the initial control vertices and a constant that depends on the valence of the patch. An efficient subdivision depth estimation technique is also proposed. Test results show that a limit mesh approximates the limit surface better than the corresponding control mesh in general.

The bounds achieved are still upper bounds, not necessarily strict. In future work we hope to derive an accurate error measure with a technique similar to Wu et al's [4, 5]. Besides the parametric distance, the bounds of other distances, such as the Hausdorff distance, are yet to be investigated.

Acknowledgments. We would like to thank the anonymous reviewers for their comments. This work was supported by the 973 Program of China (2004CB719403), NSF of China (60573151, 60473100), the 863 Program of China (2006AA01Z334, 2007AA01Z318), and China Postdoctoral Science Foundation (20060390359).

References

1. Loop, C.T.: Smooth Subdivision Surfaces Based on Triangles. M.S. Thesis, Department of Mathematics, University of Utah (1987)
2. Lanquetin, S., and Neveu, M.: A Priori Computation of the Number of Surface Subdivision Levels. In: Proceedings of International Conference on Computer Graphics and Vision 2004 (Graphicon'2004), pp. 87–94 (2004)

3. Wang, H., Sun, H., and Qin, K.: Estimating Recursion Depth for Loop Subdivision, International Journal of CAD/CAM 4:1, 11–18 (2004)
4. Wu, X., and Peters, J.: Interference Detection for Subdivision Surfaces. Computer Graphics Forum 23:3, 577–585 (2004)
5. Wu, X., and Peters, J.: An Accurate Error Measure for Adaptive Subdivision Surfaces. In: Proceedings of International Conference on Shape Modeling and Applications 2005 (SMI'05), pp. 51–56 (2005)
6. Huang, Z.: Estimating Error Bounds and Subdivision Depths for Loop Subdivision Surfaces. Technical report (availabe at `http://www.graphics.pku.edu.cn/hzj/pub/tr-loop-2007.pdf`), Peking University (2007)
7. Huang, Z., and Wang, G.: Distance Between a Catmull-Clark Subdivision Surface and Its Limit Mesh. In: Proceedings of the 2007 ACM Symposium on Solid and Physical Modeling (SPM'07), pp. 233–240 (2007)
8. Hoppe, H., DeRose, T., Duchamp, T., Halstead, M., Jin, H., McDonald, J., Schweitzer, J., Stuetzle, W.: Piecewise Smooth Surface Reconstruction. In: Proceedings of SIGGRAPH 94, pp. 295–302. ACM, New York (2004)
9. Stam, J.: Evaluation of Loop Subdivision Surfaces. In: Subdivision for Modeling and Animation, SIGGRAPH 1999 Course Notes (1999)
10. Lai, M.J.: Fortran Subroutines For B-Nets of Box Splines on Three- and Four-Directional Meshes. Numerical Algorithms 2, 33–38 (1992)
11. Farin, G.: Curves and Surfaces for CAGD — A Practical Guide, 5th Edition. Morgan Kaufmann Publishers, San Francisco (2002)

Appendix 1: Conversion Matrix T

The 15×12 matrix T which converts from the 12 control vertices of a quartic box spline surface patch to the 15 Bézier points of the corresponding quartic triangular Bézier patch is as follows:

$$T = \frac{1}{24}\begin{bmatrix}
2 & 2 & 2 & 12 & 2 & 0 & 2 & 2 & 0 & 0 & 0 & 0 \\
1 & 0 & 3 & 12 & 1 & 0 & 4 & 3 & 0 & 0 & 0 & 0 \\
0 & 1 & 1 & 12 & 3 & 0 & 3 & 4 & 0 & 0 & 0 & 0 \\
0 & 0 & 4 & 8 & 0 & 0 & 8 & 4 & 0 & 0 & 0 & 0 \\
0 & 0 & 1 & 10 & 1 & 0 & 6 & 6 & 0 & 0 & 0 & 0 \\
0 & 0 & 0 & 8 & 4 & 0 & 4 & 8 & 0 & 0 & 0 & 0 \\
0 & 0 & 3 & 4 & 0 & 1 & 12 & 3 & 0 & 0 & 1 & 0 \\
0 & 0 & 1 & 6 & 0 & 0 & 10 & 6 & 0 & 0 & 1 & 0 \\
0 & 0 & 0 & 6 & 1 & 0 & 6 & 10 & 0 & 0 & 1 & 0 \\
0 & 0 & 0 & 4 & 3 & 0 & 3 & 12 & 1 & 0 & 1 & 0 \\
0 & 0 & 2 & 2 & 0 & 2 & 12 & 2 & 0 & 2 & 2 & 0 \\
0 & 0 & 1 & 3 & 0 & 0 & 12 & 4 & 0 & 1 & 3 & 0 \\
0 & 0 & 0 & 4 & 0 & 0 & 8 & 8 & 0 & 0 & 4 & 0 \\
0 & 0 & 0 & 3 & 1 & 0 & 4 & 12 & 0 & 0 & 3 & 1 \\
0 & 0 & 0 & 2 & 2 & 0 & 2 & 12 & 2 & 0 & 2 & 2
\end{bmatrix}$$